Research in Astron. Astrophys. **2010** Vol. **10** No. **6**, 553–568
http://www.raa-journal.org *http://www.iop.org/journals/raa*

***R**esearch in*
***A**stronomy and*
***A**strophysics*

Resonant cyclotron scattering in pulsar magnetospheres and its application to isolated neutron stars *

Hao Tong[1], Ren-Xin Xu[2], Qiu-He Peng[1] and Li-Ming Song[3]

[1] Department of Astronomy, Nanjing University, Nanjing 210093, China; *haotong@nju.edu.cn*
[2] Department of Astronomy, Peking University, Beijing 100871, China
[3] Institute of High Energy Physics, Chinese Academy of Sciences, Beijing 100049, China

Received 2010 January 23; accepted 2010 March 1

Abstract Resonant cyclotron scattering (RCS) in pulsar magnetospheres is considered. The photon diffusion equation (Kompaneets equation) for RCS is derived. The photon system is modeled three dimensionally. Numerical calculations show that there exist not only up scattering but also down scattering of RCS, depending on the parameter space. RCS's possible applications to spectral energy distributions of magnetar candidates and radio quiet isolated neutron stars (INSs) are pointed out. The optical/UV excess of INSs may be caused by the down scattering of RCS. The calculations for RX J1856.5–3754 and RX J0720.4–3125 are presented and compared with their observational data. In our model, the INSs are proposed to be normal neutron stars, although the quark star hypothesis is still possible. The low pulsation amplitude of INSs is a natural consequence in the RCS model.

Key words: radiation mechanism: nonthermal — scattering — stars: neutron — pulsars: general — pulsars: individual(RX J1856.5–3754, RX J0720.4–3125)

1 INTRODUCTION

Three kinds of pulsar-like objects have greatly increased our knowledge about pulsar magnetospheres. They are anomalous X-ray pulsars and soft gamma-ray repeaters (magnetar candidates), radio quiet isolated neutron stars (INSs) (the magnificent seven), and rotating radio transients (RRATs). Figure 1 shows their positions on the $P - \dot{P}$ diagram. Our conventional picture of pulsar magnetospheres is provided by e.g. Goldreich & Julian (1969), Ruderman & Sutherland (1975), and Cheng et al. (1986) (for a recent review, see Kaspi et al. 2006), which is mainly about the open field line regions (OFLRs). Few people have begun to realize that there could be interesting physics in the closed field line regions (CFLRs) of pulsar magnetospheres. For magnetars, it is proposed that there is a strong and twisted magnetic field around the central star (Thompson et al. 2002; Lyutikov & Gavriil 2006). INSs are thought to be dead neutron stars, which provide clear specimens for magnetospheric and cooling studies (Kaspi et al. 2006; Tong & Peng 2007; Tong et al. 2008). For RRATs, recent modeling also indicates interesting physics in CFLRs (Luo & Melrose 2007). The most direct evidence comes from observations of the double pulsar system PSR J0737–3039A/B, and there could also be signatures of interesting physics in CFLRs of normal pulsars (Lyutikov 2008).

* Supported by the National Natural Science Foundation of China.

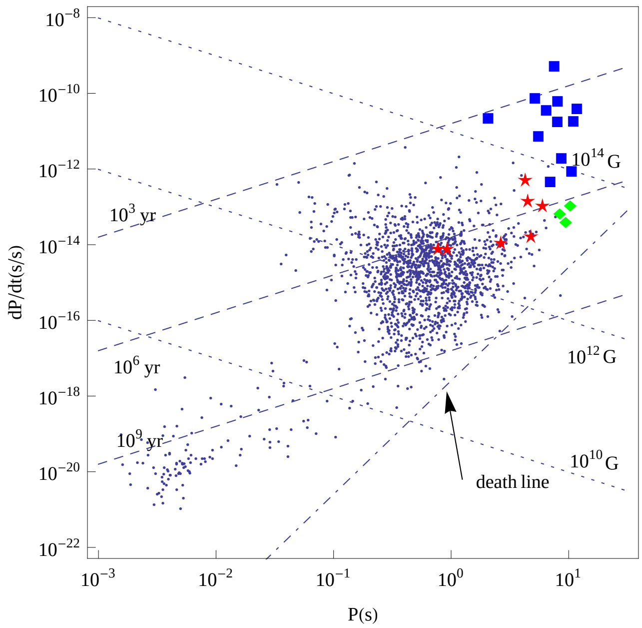

Fig. 1 $P - \dot{P}$ diagram of pulsars. Diamonds are for INSs (Haberl 2007; Kaplan & van Kerkwijk 2009). Stars are for RRATs (McLaughlin et al. 2006; McLaughlin et al. 2009). Magnetar (*squares*) and radio pulsar (*dots*) data are from ATNF (*http://www.atnf.csiro.au/research/pulsar/psrcat/*). The dot-dashed line is the constant potential line $V = 1/3 \times 10^{12}$ V.

The interesting physics in pulsar CFLRs is mainly related to the plasmas there. Roughly speaking, the electron density in magnetar CFLRs is about 4–5 orders higher than the Goldreich-Julian density (Rea et al. 2008). In the case of RRATs, Luo & Melrose (2007) have proposed the idea of a "pulsar radiation belt," like the radiation belt of the earth. Noting the similarities between INSs and magnetars/RRATs, we suggest that there could also be plasmas in INS CFLRs with number density much higher than the Goldreich-Julian density (i.e. the electron blanket, see Wang et al. 1998; Ruderman 2003). We observed three similarities between INSs and magnetars/RRATs:

1. Most of them are long period pulsars with spin periods of about 10 s;
2. They all show a non-atomic blackbody spectrum;
3. They all have large or relatively large spin-down rates (indicating possible higher fields).

With these similarities, we suggest that the physics of these three kinds of objects should be similar, and that the very different observational manifestations could have resulted from a different parameter space and an evolution history.

In this paper, we consider the resonant cyclotron scattering (RCS) process in pulsar magnetospheres. In Section 2, a brief description of the RCS process and some basic formulae are given. The Kompaneets equation for the RCS process is derived in Section 3. Numerical calculations are given in Section 4. The application to INSs is the topic of Section 5. In the last two sections, discussions and conclusions are given, respectively.

2 RESONANT CYCLOTRON SCATTERING

Near the neutron star surface, RCS of photons is more important than Compton scattering (Ruderman 2003). It has the following three points:

1. Given a magnetic field, the scattering occurs only at a specific frequency and vice versa. Given a frequency, the scattering occurs only at a specific location in the pulsar magnetosphere. At the resonant frequency, the cross section is about 8 orders larger than the Thomson cross section for a typical magnetic field of 10^{12} G.
2. The momentum is conserved only along the z-direction (direction of the magnetic field). The field may absorb or contribute to perpendicular momentum.
3. The particle distribution is strongly affected by the field. The perpendicular motion is suppressed while particles can move freely along field lines. Therefore the electron distribution is 1D.

The soft X-ray spectrum of magnetars may be the result of RCS of surface thermal emission (Rea et al. 2008). There are three ways of dealing with scattering problems (including resonant scattering). One is solving the radiation transfer equation directly (e.g. Lyutikov & Gavriil 2006), the second is doing Monte Carlo simulations (Fernandez & Thompson 2007; Nobili et al. 2008), and the third is introducing a photon diffusion equation (Kompaneets equation) as in the Compton scattering case (e.g. Rybicki & Lightman 1979). However, the Kompaneets equation for RCS has not yet been developed. Considering its importance in magnetar soft X-ray emission, we present a Kompaneets equation method for the RCS process in this paper. Also, improved approximations are employed. We find that it may account for the optical/UV excess of INSs.

The previous solution provided by Lyutikov & Gavriil (2006) has three problems which should be improved. The three problems are:

1. It is a one dimensional treatment. Photons can only propagate forward or backward. All the calculations and arguments there are valid only in the 1D case. This will cause two additional problems.
2. The angular dependence of the RCS cross section is smeared out. The rigorous expression is Equation (3) which we will discuss in the following.
3. The down scattering of photons is dropped. In the 1D case, the phase space volume is proportional to p, while in the 3D case it is proportional to p^3. Noting that photons are bosons, the key difference between the 3D and 1D cases is that there is no Bose-Einstein condensation in the latter case (Pathria 2003). The down scattering is Bose-Einstein condensation of photons in the low energy state (Liu et al. 2004; Sunyaev & Titarchuk 1980), therefore it cannot be handled in the 1D case. Then it is not surprising that the authors found a net up scattering of transmitted flux. Their approximations are the important aspect in this case. We try to provide a 3D treatment of the photon system in this paper.

Before proceeding to the details of the derivation, some basic formulae should first be given (You et al. 1997). The cyclotron frequency of electrons in a given magnetic field is

$$\nu_B = \frac{1}{2\pi}\frac{eB(r)}{m_{\rm e}c}, \tag{1}$$

$$\omega_B = \frac{eB(r)}{m_{\rm e}c}, \tag{2}$$

where ν_B is the local cyclotron frequency, ω_B is the angular frequency $\omega_B = 2\pi\nu_B$, e is the electron charge (absolute value), $B(r)$ is the local magnetic field, r is the distance from the point to the center of the star, $m_{\rm e}$ is the electron rest mass, and c is the speed of light. When $\nu = \nu_B$, where ν is the photon frequency, RCS occurs. The differential cross section is

$$d\sigma_{\rm RCS} = \frac{3r_{\rm e}c}{32}(1+\cos^2\theta)(1+\cos^2\theta')\phi(\nu-\nu_B)d\Omega', \tag{3}$$

where $r_{\rm e}$ is the classical electron radius, θ is the angle between the incoming photon and the local magnetic field, θ' denotes the angle of the outgoing photon, $d\Omega'$ is the solid angle of the outgoing photon, and $\phi(\nu-\nu_B)$ is the Lorentz line profile function, which acts like a Dirac delta function

$$\phi(\nu-\nu_B)=\frac{\Gamma/4\pi^2}{(\nu-\nu_B)^2+(\Gamma/4\pi)^2}\,. \tag{4}$$

Note that Γ is the natural width

$$\Gamma=\frac{4e^2\omega_B^2}{3m_{\rm e}c^3}\,. \tag{5}$$

The Lorentz line profile function has the normalization condition

$$\int_{-\infty}^{+\infty}\phi(\nu-\nu_B)d\nu=1\,. \tag{6}$$

Performing the angular integral gives the total cross section

$$\sigma_{\rm RCS}=\frac{1}{2}\pi r_{\rm e}c(1+\cos^2\theta)\phi(\nu-\nu_B)\,, \tag{7}$$

which depends on frequency.

In the case of pulsars, a dipole magnetic field is always a good approximation. The magnetic field at radius r is

$$B(r)=B_p\left(\frac{R}{r}\right)^3\,, \tag{8}$$

where B_p is the magnetic field at the surface of the neutron star, and R is the neutron star radius. Given a photon frequency ν, the radius at which RCS occurs is

$$r_{\rm RCS}=\left(\frac{\nu_{B_p}}{\nu}\right)^{1/3}R\,, \tag{9}$$

where ν_{B_p} is the cyclotron frequency at the star's surface $\nu_{B_p}=\frac{1}{2\pi}\frac{eB_p}{m_{\rm e}c}$ (only photons with frequencies smaller than ν_{B_p} will encounter RCS). For photons in the soft X-ray band $1\,{\rm keV}<h\nu<10\,{\rm keV}$ (where h is Planck's constant), we are only considering a specific frequency range $\nu_1<\nu<\nu_2$. The scattering occurs in a finite space range $r_2<r<r_1$, where r_2 is the scattering radius corresponding to frequency ν_2, and r_1 corresponds to frequency ν_1. We assume that there is a bulk of electrons filling the space between r_2 and r_1. Beyond r_1, there may also be a bulk of electrons, but it is less related to the observations in the frequency range ν_1 to ν_2. Finally, we introduce the optical depth of RCS

$$\tau_{\rm RCS}=\int N_{\rm e}\sigma_{\rm RCS}dr=\tau_0(1+\cos^2\theta)\,, \tag{10}$$

where $N_{\rm e}$ is the electron number density (assuming homogeneity),

$$\tau_0=\frac{\pi e^2N_{\rm e}r_{\rm RCS}}{6m_{\rm e}c\,\nu}\,. \tag{11}$$

The optical depth also depends on frequency $\propto 1/\nu^{4/3}$. In the following sections, all optical depths are referred to by their value at the lower frequency boundary, i.e. optical depth at ν_1. During the integration of Equation (10), the spatial dependence of the magnetic field (Eq. (8)) is taken into consideration. This will be used in the numerical calculation section.

3 KOMPANEETS EQUATION FOR RESONANT CYCLOTRON SCATTERING

We formulate our derivation to be analogous to that of the Kompaneets equation for Compton scattering (e.g. Rybicki & Lightman 1979; You 1998; Padmanabhan 2000).

Denote the initial and final state of the scattering as $(p_z,\ \nu,\ \boldsymbol{n})$ and $(p'_z,\ \nu',\ \boldsymbol{n}')$, respectively, where p_z is the initial electron momentum in the z-direction, ν the initial photon frequency, $\boldsymbol{n}$ the propagation direction of the incoming photon, and a prime denotes the corresponding quantity of the outgoing particles. In a strong magnetic field, electron motions which are perpendicular to the magnetic field are trapped into Landau energy levels. Almost all the electrons are in the ground state (You et al. 1997). Thus, we only consider photons in the ground state before and after the scattering (Herold 1979). According to energy-momentum conservation in the non-relativistic case, we have

$$h\nu + \frac{p_z^2}{2m_{\rm e}} \ = \ h\nu' + \frac{p_z'^2}{2m_{\rm e}}, \tag{12}$$

$$\left(\frac{h\nu}{c}\cos\theta\right) + p_z \ = \ \left(\frac{h\nu'}{c}\cos\theta'\right) + p'_z\,. \tag{13}$$

It seems that we are dealing with a 1D distribution of electrons.

From the conservation of energy and momentum, we can calculate the frequency change after and before the scattering $\Delta = h(\nu' - \nu)/kT_{\rm e}$, with k being Boltzmann's constant, and $T_{\rm e}$ the temperature of the electron system. Since we are dealing with non-relativistic electrons $kT_{\rm e} \ll m_{\rm e}c^2$, and we consider typical photons in the X-ray band $h\nu \sim 1\,{\rm keV} \ll m_{\rm e}c^2$, the frequency change is very small $\Delta \ll 1$. Therefore only considering the first order terms of Δ, we have

$$\Delta = -\frac{xp_z}{m_{\rm e}c}(\cos\theta - \cos\theta')\,, \tag{14}$$

where x is the dimensionless frequency $x = h\nu/kT_{\rm e}$. The above expression is accurate to an order of $O(\frac{h\nu}{m_{\rm e}c^2}\frac{h\nu}{kT_{\rm e}})$, which is negligible in the case of magnetars and INSs. The validity of using the method based on the Kompaneets equation in the nonrelativistic case is well established (e.g. eq. (7.53) in Rybicki & Lightman 1979).

Let $n(\nu)$ denote the occupation number per photon state of frequency ν. We denote the transition probability from an initial state $(p_z,\ \nu,\ \boldsymbol{n})$ to a final state $(p'_z,\ \nu',\ \boldsymbol{n}')$ as dW. Note that because the transition probability is a microscopic quantity, we always have $dW' = dW$. Since electrons move freely along the z-direction, we describe the electron system as a 1D Maxwellian distribution. The number of electrons with momentum in the range $p_z - p_z + dp_z$ is $f(p_z)dp_z$, with

$$f(p_z) = N_{\rm e}(2\pi m_{\rm e}kT_{\rm e})^{-1/2}e^{-p_z^2/2m_{\rm e}kT_{\rm e}}\,. \tag{15}$$

The evolution of the photon spectrum is described by the Boltzmann equation (Rybicki & Lightman 1979)

$$\left(\frac{\partial n}{\partial t}\right)_{\rm RCS} = \int dp_z \int dW[f(p'_z)n'(1+n) - f(p_z)n(1+n')]\,, \tag{16}$$

where a subscript RCS means the change of occupation number caused by RCS; n and n' are abbreviated forms of $n(\nu)$ and $n(\nu')$, respectively. For non-relativistic electrons, the frequency change is small, with $\Delta \ll 1$, so we can expand Equation (16) to terms of Δ^2 and neglect higher order terms. The change of photon occupation number becomes

$$\begin{aligned}\left(\frac{\partial n}{\partial t}\right)_{\rm RCS} \ = \ & \left[\frac{\partial n}{\partial x} + n(1+n)\right]\int dp_z \int dW f(p_z)\Delta \\ & + \left[\frac{1}{2}\frac{\partial^2 n}{\partial x^2} + \frac{\partial n}{\partial x}(1+n) + \frac{1}{2}n(1+n)\right]\int dp_z \int dW f(p_z)\Delta^2\,. \end{aligned} \tag{17}$$

We denote the two integrals by

$$I_1 = \int dp_z \int dW f(p_z) \Delta \,, \tag{18}$$

$$I_2 = \int dp_z \int dW f(p_z) \Delta^2 \,, \tag{19}$$

and then Equation (17) becomes

$$\begin{aligned}\left(\frac{\partial n}{\partial t}\right)_{\rm RCS} &= \left[\frac{\partial n}{\partial x} + n(1+n)\right] I_1 \\ &+ \left[\frac{1}{2}\frac{\partial^2 n}{\partial x^2} + \frac{\partial n}{\partial x}(1+n) + \frac{1}{2}n(1+n)\right] I_2 \,. \end{aligned} \tag{20}$$

Using the property of conservation of photon number can greatly simplify the subsequent calculations.

The number of photons is conserved during the scattering process. Thus, we have the continuity equation of $n(x)$ in frequency space

$$\frac{\partial n}{\partial t} = -\nabla \cdot \boldsymbol{j} \,, \tag{21}$$

where $\boldsymbol{j}$ is the photon flux in frequency space. Assuming $n(x)$ is isotropic (the validity of the isotropic assumption will be discussed in the appendix), we have

$$\frac{\partial n}{\partial t} = -\frac{1}{x^2}\frac{\partial}{\partial x}(x^2 j) \,. \tag{22}$$

A comparison between Equations (22) and (20) shows that the flux j must have the form (Rybicki & Lightman 1979)

$$j(x) = g(x)\left[\frac{\partial n}{\partial x} + n(1+n)\right] \,. \tag{23}$$

Note that in equilibrium conditions, $n(x) = (e^x - 1)^{-1}$, $\frac{\partial n}{\partial x} = -n(1+n)$, and we have no "photon flux" in frequency space, with $j = 0$. This is a necessary condition. The same condition can be used to check the validity of other forms of the diffusion equation (e.g. Liu et al. 2004). Substituting the above equation into Equation (22), we have

$$\frac{\partial n}{\partial t} = -\frac{1}{x^2}\frac{\partial}{\partial x}\left\{x^2 g(x)\left[\frac{\partial n}{\partial x} + n(1+n)\right]\right\} \,. \tag{24}$$

A comparison between the coefficient of $\frac{\partial^2 n}{\partial x^2}$ in Equations (24) and (20) gives $g(x)$

$$g(x) = -\frac{1}{2} I_2 \,. \tag{25}$$

Finally, the Kompaneets equation for RCS has the form

$$\frac{\partial n}{\partial t} = \frac{1}{x^2}\frac{\partial}{\partial x}\left\{x^2 \frac{1}{2} I_2 \left[\frac{\partial n}{\partial x} + n(1+n)\right]\right\} \,. \tag{26}$$

We only need to calculate the integral I_2.

Substituting the equation of frequency change Equation (14) into the definition of the integral I_2 in Equation (19) and first performing the integral of momentum p_z, we obtain

$$I_2 = \int dW x^2 N_{\rm e} \frac{kT_{\rm e}}{m_{\rm e}c^2}(\cos\theta - \cos\theta')^2 \,. \tag{27}$$

The transition probability is directly related to cross section

$$\begin{aligned} dW &= c d\sigma_{\rm RCS} \\ &= c\frac{3r_{\rm e}c}{32}(1+\cos^2\theta)(1+\cos^2\theta')\phi(\nu-\nu_B)d\Omega' \,. \end{aligned} \tag{28}$$

Since we are dealing with non-relativistic electrons, the cross section can be approximated by its value in the electron rest frame. Performing the integral over $d\Omega'$, we have

$$I_2 = 2x^2 N_{\rm e}\sigma_{\rm RCS}\, c\frac{kT_{\rm e}}{m_{\rm e}c^2}g_\theta \,, \tag{29}$$

where g_θ is an angle dependent factor $g_\theta = \frac{1}{5} + \frac{1}{2}\cos\theta^2$. Finally, the Kompaneets equation for RCS is

$$\left(\frac{\partial n}{\partial t}\right)_{\rm RCS} = \frac{kT_{\rm e}}{m_{\rm e}c^2}\frac{1}{x^2}\frac{\partial}{\partial x}\left\{x^4 N_{\rm e}\sigma_{\rm RCS}\, c\, g_\theta\left[\frac{\partial n}{\partial x}+n(1+n)\right]\right\} \,. \tag{30}$$

The cross section $\sigma_{\rm RCS}$ now depends on frequency, therefore it cannot be taken out of the curly brackets. Except for this difference and an angle dependent factor g_θ, it is the same as the Kompaneets equation for Compton scattering.

4 NUMERICAL CALCULATIONS

Before we make numerical calculations of Equation (30), two integrations should be performed. Performing a space integral on both sides of Equation (30), which employs the concept of optical depth as in Equation (10), we obtain the Kompaneets equation that can be used in the case of pulsars

$$\left(\frac{\partial n}{\partial t}\right)_{\rm RCS} = \frac{kT_{\rm e}}{m_{\rm e}c^2}\frac{1}{x^2}\frac{\partial}{\partial x}\left\{x^4 \frac{\tau_{\rm RCS}}{r_1-r_2} c\, g_\theta\left[\frac{\partial n}{\partial x}+n(1+n)\right]\right\} \,. \tag{31}$$

The expresssion $r_1 - r_2$ in the denominator is the range of integration. It is also the range of cyclotron scattering corresponding to the frequency range ν_1 to ν_2. The space integration must be employed in order to eliminate the Dirac delta function in the RCS cross section.

There is an angular factor in the RCS optical depth $\tau_{\rm RCS}$, and we denote it as $f_\theta = 1+\cos^2\theta$. To simplify the calculations, we use the average value of f_θ and g_θ

$$\overline{f_\theta} = \frac{4}{3} \,, \tag{32}$$

$$\overline{g_\theta} = \frac{2}{5} \,. \tag{33}$$

Here $\overline{g_\theta} = \overline{f_\theta g_\theta}/\overline{f_\theta}$. From Equation (30) till now, we have performed two integrations. One is an integration over the space range, the other is averaging over the incoming angle. These two integrations are introduced in order to simplify the numerical calculations.

The Kompaneets equation for RCS is a pure initial value nonlinear partial differential equation. Solving the pure initial value problem follows the same routine as the mixed initial value and boundary value problem. In the case of the Kompaneets equation for RCS, we have to be careful since we are working in a semi-infinite domain, which is $0 < \nu < \infty$. In the real case, we are only interested in a finite frequency range (e.g. in the cases of magnetars, INSs). Therefore boundary conditions are needed.

The Kompaneets equation for RCS describes the diffusion of photons in frequency space. It is related to the specific intensity as

$$I_\nu(t) = \frac{2h\nu^3}{c^2}n(\nu,t) \,. \tag{34}$$

For a blackbody spectrum, the initial condition is[1]

$$n(x, t = 0) = \frac{1}{\exp(\frac{x}{T_{\rm rad}/T_{\rm e}}) - 1}\,. \qquad (35)$$

Since we only consider pure scattering between electrons and photons, the number of photons is conserved. The choice of boundary conditions must guarantee this requirement. One guess is that there are no photons going in or out of the specified frequency range. Mathematically this is

$$\frac{\partial n(x,t)}{\partial x} + n(x,t)[1 + n(x,t)] = 0, \quad \text{when } x = x_1,\ x_2 \quad \text{for all } t\,. \qquad (36)$$

Compare this expression to Equation (23) (Ross et al. 1978). During the numerical calculations, a simplified version is used[2]

$$\frac{\partial n(x,t)}{\partial x} = 0, \text{when } x = x_1,\ x_2 \quad \text{for all } t\,. \qquad (37)$$

In obtaining the final RCS modified spectrum, we use the random walk approximation. A photon entering the lower boundary r_2 escapes the outer boundary r_1 after an average diffusion time scale

$$t_{\rm dif} = \tau_{\rm RCS}(\nu_1)(r_1 - r_2)/c\,. \qquad (38)$$

In the random walk approximation, $n(x, t_{\rm dif})$ is the final output.

Figures 2 and 3 are the numerical results for the up scattering and down scattering case, respectively. Figure 2 shows the result for typical parameters of magnetars. During the calculations, the magnetic field and stellar radius are chosen as typical values of $B = 4.4\times10^{14}$ G and $R = 10^6$ cm. It can reproduce a stiffened blackbody spectrum, therefore it may be applied to interpreting a magnetar soft X-ray spectrum. Figure 3 shows the calculation for typical parameters of INSs with $B = 10^{13}$ G and $R = 10^6$ cm. It produces a spectrum with optical/UV excess. Therefore it may account for the optical/UV excess of INSs.

The luminosity of photons[3] (number of photons per unit time passing a fixed surface) is proportional to $\int_{x_1}^{x_2} x^2 n(x,t)\,dx$. We can calculate this integral before and after the scattering to check whether the number of photons is conserved during the calculations. In the down scattering case, the specified frequency range spans about three orders of magnitude. The number of photons changes by less than five percent before and after the scattering. While in the up scattering case, the specified frequency range only spans one order of magnitude. If we insert boundary conditions at x_1 and x_2, the number of photons is not conserved. It is because the specified frequency range is not wide enough. Therefore, we insert boundary conditions "far away" from the specified frequency range, at $x_1/10$ and $15\,x_2$. The number of photons changes by less than one thousandth.

---

[1] We are considering a spherical shell of electrons, extending from r_2 to r_1. When the radiation reaches the lower boundary r_2, this is taken as $t = 0$. At r_2, it is already several radii away from the neutron star surface. The gravity there is already very weak. Therefore, the general relativistic effect is negligible when the radiation propagates from r_2 to r_1.

[2] Take the equilibrium condition, for example, $n(\nu) = \frac{1}{e^{h\nu/kT_{\rm rad}} - 1}$. At the upper frequency boundary $h\nu_2 \gg kT_{\rm rad}$, $n \ll 1$, the third type of boundary condition is reduced to the second type. At the lower boundary $h\nu_1 \leq kT_{\rm rad}$, this is a poor approximation. However, the number of low energy photons is proportional to $x^2 n(x)dx \propto x^2 \ll 1$, which is also a small amount. Therefore, we employ the simplified version of boundary conditions. The validity of this simplified approximation is discussed at the end of this section.

[3] luminosity=flux$\times$ area=$\pi \frac{I_\nu}{h\nu} \left(\frac{R}{r}\right)^2 4\pi r^2$, then integrate over the specified frequency range.

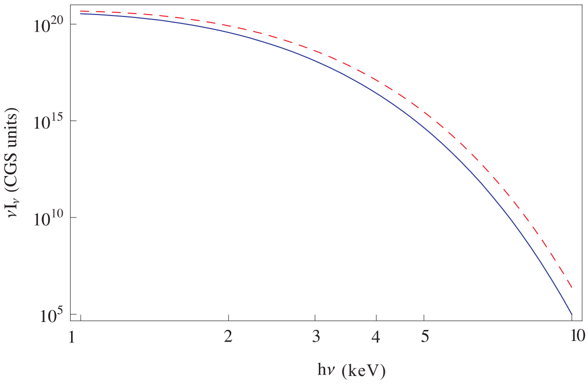

Fig. 2 Modified blackbody spectrum due to resonant cyclotron scattering (up scattering case) for typical parameters of magnetars. The initial blackbody temperature is $0.2\,\text{keV}$, the electron temperature is $10\,\text{keV}$. The solid line is the initial blackbody spectrum. The dashed line is the RCS modified spectrum with an optical depth $\tau_{\text{RCS}}(\nu_1) = 2$. The specified frequency range is $(\nu_1, \nu_2) = (1\,\text{keV}, 10\,\text{keV})$. The model parameters are $(x_1, x_2) = (0.1, 1)$, $(r_2, r_1) = (8.0, 17) \times 10^6\,\text{cm}$.

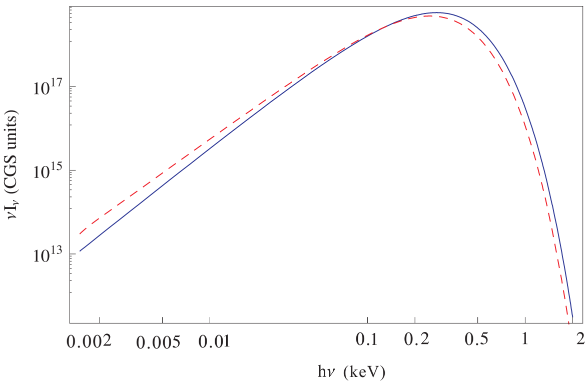

Fig. 3 Modified blackbody spectrum due to resonant cyclotron scattering (down scattering case) for typical parameters of isolated neutron stars. The initial blackbody temperature is $70\,\text{eV}$, the electron temperature is $26\,\text{eV}$. The solid line is the initial blackbody spectrum. The dashed line is the RCS modified spectrum with an optical depth $\tau_{\text{RCS}}(\nu_1) = 1000$. The specified frequency range is $(\nu_1, \nu_2) = (1.5\,\text{eV}, 2\,\text{keV})$. The model parameters are $(x_1, x_2) = (0.058, 77)$, $(r_2, r_1) = (3.9, 42) \times 10^6\,\text{cm}$.

5 APPLICATION TO ISOLATED NEUTRON STARS

ROSAT discovered seven radio quiet INSs (Kaspi et al. 2006; Trümper 2005; for recent reviews see Haberl 2007; van Kerkwijk & Kaplan 2007). They all show featureless blackbody spectra, with low pulsation amplitude, and high X-ray to optical flux ratio. Their spectral energy distributions show that many of them have an optical/UV excess with a factor of several times (Burwitz et al. 2001; Burwitz et al. 2003; Motch et al. 2003; Ho et al. 2007; van Kerkwijk & Kaplan 2007). Table 1 shows double blackbody fits of RX J1856.5–3754 (J1856 for short) and RX J0720.4–3125 (J0720 for

Table 1 Double Blackbody Fit to INS Spectral Energy Distributions

	kT_X (eV)	R_X (km)	kT_O (eV)	R_O (km)	distance (pc)
J1856	63	5.9	26	24.3	161
J0720	85.7	5.7	35.4	23.5	330

Notes: T_X is the high temperature component (X-ray), and T_O is the low temperature component (optical/UV), seen at infinity. R_X and R_O are the corresponding emission radii, seen at infinity. Here all numbers are only estimated values, and no error bars are given, which are taken from van Kerkwijk & Kaplan (2007).

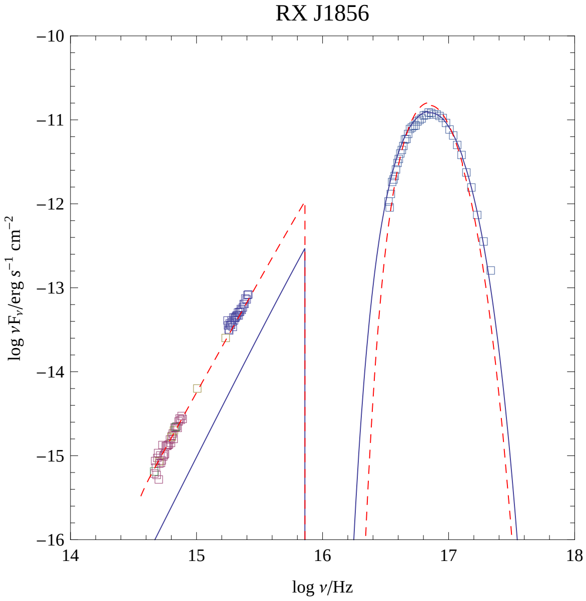

Fig. 4 Spectral energy distributions of J1856. The squares are observational points (only central values are included). The solid line is a single blackbody fit to the X-ray data whose parameters are given in Table 1. (It is not the initial blackbody spectrum in our model, and the parameters are listed in Table 2.) The dashed line is the RCS modified blackbody spectrum whose model parameters are given in Table 2. The specified frequency range and model parameters are the same as those in Fig. 3. All observational data are from van Kerkwijk & Kaplan (2007).

short). In interpreting their optical/UV excess, the emission radius is either too small or too big for a reasonable star radius. Several theoretical models have been proposed (Motch et al. 2003; Ho et al. 2007; Trümper 2005). Considering the discrepancy between current theory and observations, we try to provide an alternative one, in which the optical/UV excess of INSs may be due to magnetospheric processes, i.e. due to down scattering of RCS when the surface emission is passing through the pulsar magnetosphere.

Figures 4 and 5 show the RCS modified blackbody spectra in the cases of J1856 and J0720, respectively. These can account for the optical/UV excess in J1856 and J0720 quite well. We assume that the initial spectrum is a blackbody. When passing through the pulsar magnetosphere, it is modified by the RCS process. Therefore, the final observed spectrum is a modified blackbody, with an optical/UV excess due to down scattering of RCS. Four parameters are needed: the initial

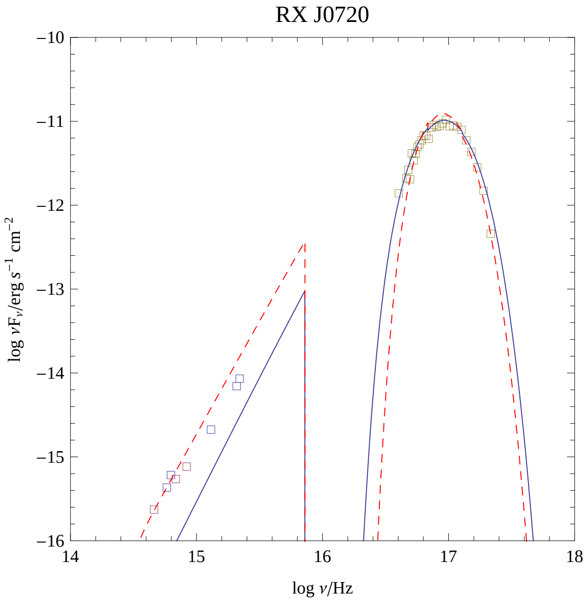

Fig. 5 Spectral energy distributions of J0720 similar to Fig. 4. The optical/UV data of J0720 is more likely to be nonthermal. The specified frequency range is the same as that in Fig. 3. The model parameters are $(x_1, x_2) = (0.042, 56)$, $(r_2, r_1) = (3.9, 42) \times 10^6$ cm. (The space range is the same as that in Fig. 3, since it is only determined by the specified frequency range, see Eq. (9)). All observational data are from van Kerkwijk & Kaplan (2007).

Table 2 RCS Fit to INS Spectral Energy Distributions

	$kT_{\rm rad}$ (eV)	$kT_{\rm e}$ (eV)	$N_{\rm e}$ (10^{12} cm^{-3})	norm	$n_{\rm H}$ (10^{20} cm^{-2})
J1856	61	26	1.8	$\pi(10\,{\rm km}/161{\rm pc})^2$	1.6
J0720	80	35.4	1.8	$\pi(10\,{\rm km}/330{\rm pc})^2$	2.8

Notes: $T_{\rm rad}$ is the initial blackbody temperature, and $T_{\rm e}$ is the temperature of the electron system, seen at infinity. $N_{\rm e}$ is the electron number density, and "norm" is the solid angle of the source seen by the observer. The equivalent hydrogen column density $n_{\rm H}$ is the result of the wabs model.

blackbody temperature, the temperature of the electron system, the electron number density (assuming homogeneity), and a normalization constant. We point out that our model has the same number of free parameters as the double blackbody fit (two temperatures and two normalization constants). The RCS model parameters are given in Table 2.

During the fitting process, the magnetic field and stellar radius are chosen to have typical values of 10^{13} G and 10 km, respectively (e.g. Haberl 2007). In the case of J1856, the initial blackbody temperature is chosen to be slightly lower than the high temperature component of the double blackbody fit. The temperature of the electron system is chosen as the low temperature component of the double blackbody fit and kept fixed during the fitting process. The electron number density is assumed to be homogenous. The corresponding optical depth is about 1000. The normalization constant is the solid angle of the source seen by the observer. The photoelectric absorption cross section is from

Morrison & McCammon (1983) (the wabs model). The hydrogen column density is consistent with previous studies (Burwitz et al. 2003; Ho et al. 2007).

The case of J0720 is similar. This may in part reflect the similarities between these two INSs. The optical/UV excess of INSs in our model is due to magnetospheric processes. This means that, in our model, the central star can be a normal neutron star, although other possibilities, e.g. a quark star, cannot be ruled out (Xu 2002, 2003; for a review, see Xu 2009).

In our model of the INSs, the blackbody spectrum is from the whole stellar surface. When passing through the CFLRs of the pulsar magnetosphere, the photons are down scattered by the RCS process. It will cause a decrease of high energy photons. This can account for the observed optical/UV excess. At the same time, since the X-ray emission is from the whole stellar surface, it can also naturally explain the low pulsation amplitude.

6 DISCUSSION

We consider the RCS process in this paper. Previous work of Ruderman (2003) mainly has a qualitative consideration, while our paper is a quantitative one and detailed comparison with observational data is also presented. Lyutikov & Gavriil (2006) consider the RCS process by solving the radiation transfer equation directly. We point out the differences between our paper and theirs.

1. An improved approximation is used. The photon system is modeled three dimensionally in our paper.
2. A different method is employed. While Lyutikov & Gavriil solved the radiation transfer equation directly, we employed the Kompaneets equation method. They are independent methods. The Kompaneets equation method is much simpler both analytically (compared to solving the radiation transfer equation directly; this is why we can employ better approximations) and numerically (compared to doing Monte Carlo simulations).
3. Different applications are considered. Previous researchers on RCS mainly focus on its application to magnetars. We point out that it may also play an important role in the radio quiet INS case. Therefore, a magnetospheric model is presented for the optical/UV excess of INSs.
4. Our calculations show that there exist not only up scattering but also down scattering of the RCS process.

Further Monte Carlo simulations may tell us more about the down scattering of RCS if there exists real down scattering of RCS. The approximation of a 1D treatment (Lyutikov & Gavriil 2006) may result in a negative point of down scattering of RCS. Our derivation is in the 3D case (for the photon system). The key difference is the phase space volume (in the 1D case $\propto p$, in the 3D case $\propto p^3$). In Equation (16), we note that a factor $(1 + n)$ appears. This is a pure second quantization effect. The photons are aligned to condense in the low energy state, and this quantum effect can only play an important role in the 3D case. Note that there is also no Bose-Einstein condensation in the low dimensional case (see Pathria 2003).

Throughout this paper, we talk about the RCS process in pulsar magnetospheres. We think it may be a common process. In different cases, it has different manifestations. In the case of magnetars, we have observed a stiffened blackbody spectrum. In the case of INSs, we have observed an optical/UV excess. These different manifestations can be treated universally using the Kompaneets equation for the RCS presented in this paper.

Concerning the magnetospheric properties, now people are thinking that the CFLRs of pulsar magnetospheres are not dead but filled with dense plasma (Ruderman 2003; Luo & Melrose 2007; Lyutikov 2008). The plasma can be $10^4 - 10^5$ times denser than the local Goldreich-Julian density. The origin of this overdense plasma is the consequence of the presence of twisted magnetic field lines (in the case of magnetars) or magnetic mirroring (in the case of RRATs). When discussing the magnetospheric properties we have to be careful. As stated in Section 2, the scattering radius and the optical depth (or cross section) is frequency-dependent. The local Goldreich-Julian density is proportional to the magnetic field. At the scattering sphere, from Equation (1), it is proportional to the photon frequency. Given that the electron density is a constant, the ratio of $N_{\rm e}/n_{\rm GJ}$ varies with frequency as $\propto 1/\nu$. In the case of magnetars (photon energy ranges between $1\,{\rm keV} - 10\,{\rm keV}$), the electron density is $10^3 - 10^4$ times the local Goldreich-Julian density while in the case of INSs, we have a broader frequency range $1\,{\rm eV} - 1\,{\rm keV}$ and a much higher RCS optical depth, about 1000. The corresponding electron density is $10^3 - 10^6$ times the local Goldreich-Julian density. Therefore, a plasma with number density $10^4 - 10^5$ times the local Goldreich-Julian density is presented in the CFLRs of magnetars/INSs according to our model. We have computed the mass of this dense plasma. Assuming an electron-ion plasma, the total mass is 10^{11} g and 10^{12} g in the magnetar case and INS case, respectively. This is consistent with studies in the double pulsar binary PSR J0737–3039, Crab giant pulses, and magnetar spectrum modeling (Lyutikov 2008; Rea et al. 2008).

The presence of dense plasmas in CFLRs of INSs needs further explanations. Unlike the case of magnetars, the INSs are believed to be dead NSs (Kaspi et al. 2006; Trümper 2005). For slow rotators like INSs, the magnetic mirroring mechanism comes into play (Luo & Melrose 2007). Therefore, we think that the dense plasma in the case of INSs could be due to the magnetic mirroring mechanism. The source of this dense plasma may be the result of accretion from circumpulsar material, e.g. ISM, fallback disk etc. Unlike the case of RRATs, in the case of INSs the radiation belts are not very far away from the neutron stars (about 40 stellar radii at the outer edge). We may call it the "inner radiation belt" of a pulsar if we call the radiation belt near the light cylinder proposed by Luo & Melrose (2007) the "outer radiation belt" of a pulsar. Nevertheless, the particle processes are similar. The pulsar accretes material from the environment which will be accelerated in the "dormant outer gap" (Luo & Melrose 2007). High energy curvature photons will collide with surface X-ray photons generating pairs in INS CFLRs. The pair plasma will be confined by the magnetic mirroring mechanism. This is the pulsar "inner radiation belt" (or "electron blanket," e.g. Ruderman 2003). Semi-quantitative estimates are given in Luo & Melrose (2007), and Ruderman (2003). It can be as high as $10^4 - 10^5$ times the Goldreich-Julian density. The plasma is cold since it has undergone a long time of relaxation (INSs are old thermally emitting neutron stars). Meanwhile during the scattering process, the photons will push the plasma particles away from the star. The kinetic energy of the particle decreases, thus resulting in a low temperature. This also explains why the plasma system in INS CFLRs is distributed in a rather wide space range, see the caption of Figure 3. A similar process is also possible in the coronae of magnetars (Beloborodov & Thompson 2007).

The last but not least important question is: can a neutron star have a blackbody spectrum which can be modified when passing through its magnetosphere? It might not be impossible. The current neutron star atmosphere models leave us two questions: one is that a blackbody spectrum fits the observation better than that with spectral lines (Ho et al. 2007). The other is that we have not found a high energy tail in INS X-ray spectra (van Kerkwijk & Kaplan 2007). Therefore from the observational point of view, a blackbody spectrum is possible. A blackbody-like spectrum could be reproduced in a quark star model (Xu 2009).

7 CONCLUSIONS

We consider the RCS process in pulsar magnetospheres. The photon diffusion equation (Kompaneets equation) for RCS is presented. It can not only produce up scattering but also down scattering depending on the parameter space. Its possible applications to magnetar soft X-ray spectra and INSs are pointed out.

The application to INSs is calculated in detail. We show that the optical/UV excess of INSs may be due to down scattering of RCS. The RCS model has the same number of parameters as the double blackbody model. Meanwhile, it has a clear physical meaning. The initial blackbody spectrum from the stellar surface is down scattered by the RCS process when passing through its magnetosphere.

This can account for the optical/UV excess of INSs. The low pulsation amplitude of INSs is a natural consequence in our model.

The calculations for RX J1856.5–3754 and RX J0720.4–3125 are presented and compared with their observational data. The model parameters for RX J1856.5–3754 and RX J0720.4–3125 are similar. This may in part reflect the similarities between these two INSs. Finally, we point out that the quark star hypothesis (e.g. Xu 2002) still cannot be ruled out.

The photon diffusion equation (Kompaneets equation) for RCS is calculated semi-analytically. The calculations for the magnetar and INS cases are all for surface thermal emission. Of course, its application is not limited to the thermal emission case.

Using the Kompaneets equation (both the resonant and non-resonant ones, or a unified one which will be presented in the future), a thorough and quantitative study of the scattering processes in pulsar magnetospheres could be possible. This can help us make clear the physical process in CFLRs of pulsar magnetospheres.

Acknowledgements The authors would like to thank Prof. van Kerkwijk very much for providing the observational data. H.T. would like to thank Yue You Ling and Liu Dang Bo for helpful discussions. H.T. would like to thank Prof. Chou Chih-Kang very much for sharing his manuscript which is also on the Kompaneets equation for resonant cyclotron scattering. This work is supported by the National Natural Science Foundation of China (Grant Nos. 0201131077, 10935001, 10973002, 10778604 and 10773017), the Doctoral Program Foundation of the State Education Commission of China, the National Basic Research Program of China (Grant 2009CB824800), and by LCWR (LHXZ200602).

Appendix A: PROPAGATION EFFECT

The validity of the isotropic assumption employed in the main body is discussed. From Equations (21) to (22), we employ the isotropic assumption. This is also implicitly assumed during the angular average in the numerical calculation section. Its validity is acceptable in regions not far from the star. This is just the case at the inner edge r_2 of the "electron blanket." However, at the outer edge r_1, its validity needs further confirmation. Our approach to this problem is that we consider an isotropization process. From Equation (3), the angular dependence of the outgoing photons is $(1+\cos^2\theta')$, the same as that of cyclotron radiation. It is almost isotropic. Therefore, weakly dependent on the angle of incoming photons, the photons become isotropic through the RCS process. This allows the required isotropic photon field to be scattered by nearby electrons. The upper isotropization process is valid from one space location to another. Therefore, the isotropic assumption is valid through the whole space range, from r_2 to r_1.

Note that the number of photons is conserved during the scattering process. The r^{-2} dependence of the solid angle of the star is "transformed" to the photon occupation number $n(x,t)$. It will only modify the space integrated form of the Kompaneets equation, Equation (31). However, since the output is not sensitive to where we introduce the r^{-2} dependence, the results should be similar. A detailed calculation is presented below.

The energy density of the radiation field is

$$u_\nu = \frac{4\pi}{c} J_\nu, \tag{A.1}$$

where J_ν is the mean intensity

$$J_\nu = \frac{1}{4\pi}\int I_\nu d\Omega, \tag{A.2}$$

and I_ν is the specific intensity. From the definition of photon occupation number, we have

$$u_\nu = n(\nu)\frac{8\pi\nu^2}{c^3}h\nu, \tag{A.3}$$

where $n(\nu)$ is the photon occupation number in the Kompaneets equation. Combining Equations (A.1) and (A.3), we obtain the relation between mean intensity and occupation number

$$J_\nu = \frac{2h\nu^3}{c^2} n(\nu). \tag{A.4}$$

For an isotropic radiation field (e.g. as we have assumed in the main text), this is just Equation (34). We consider the propagation effect for a uniformly bright sphere with brightness B_ν and radius R (e.g., Rybicki & Lightman 1979, sect. 1.3). The mean intensity at radius r is

$$J_\nu = \frac{1}{2} B_\nu \left[1 - \sqrt{1 - (R/r)^2}\right]. \tag{A.5}$$

The dilution factor is

$$\frac{J_\nu(r \gg R)}{J_\nu(r = R)} = \frac{1}{2}\left(\frac{R}{r}\right)^2. \tag{A.6}$$

This is also the dilution factor for the occupation number $n(\nu)$.

Only considering the propagation effect, this will introduce a spatial dependence of the photon occupation number

$$\frac{\partial}{\partial r} r^2 n(\nu, r) = 0. \tag{A.7}$$

For a neutron star with surface temperature $T_{\rm rad}$, the photon occupation at radius r is

$$n(\nu, r \gg R) = \frac{1}{4} \frac{1}{e^{h\nu/kT_{\rm rad}} - 1} \left(\frac{R}{r}\right)^2. \tag{A.8}$$

Besides the dilution factor, it means that only half of the photons will propagate towards the observer.

The photon occupation number now in Equation (30) is a function of frequency, time, and position $n = n(\nu, t, r)$. In order to include the dilution effect, we introduce another variable m

$$m(\nu, t) = r^2 n(\nu, t, r). \tag{A.9}$$

From Equation (A.7), m only depends on frequency and time. Multiplying r^2 on both sides of Equation (30) and performing a spatial integral from r_2 to r_1, we obtain

$$\left(\frac{\partial m}{\partial t}\right)_{\rm RCS} = \frac{kT_e}{m_e c^2} \frac{1}{x^2} \frac{\partial}{\partial x} \left\{ x^4 \frac{\tau_{\rm RCS}}{r_1 - r_2} c\, g_\theta \left[\frac{\partial m}{\partial x} + m(1 + \frac{m}{r_{\rm RCS}^2}) \right] \right\}. \tag{A.10}$$

It is similar to Equation (31).

In order to make a comparison with the observational data, the flux of such a system must be calculated. It is related to the energy density

$$\begin{aligned} F_\nu &= u_\nu c \\ &= \frac{8\pi h\nu^3}{c^2} n(\nu, t, r) \\ &= \frac{8\pi h\nu^3}{c^2} \frac{m(\nu, t)}{D^2}, \end{aligned} \tag{A.11}$$

where D is the distance to this source. The spectrum is proportional to $\nu^3 m(\nu, t)$. Similar results are obtained with similar input parameters in the main text.

There is an important reason why the isotropic assumption is still valid in regions far away from the star. From Equation (9), low energy photons will be scattered in outer regions. At the same time, they have a large cross section and optical depth, e.g. see Equation (10) and the caption of Figure 3. Low energy photons will encounter strong scattering, although they are limited to a narrow beam. A related issue has already been pointed out in Section 2.

References

Beloborodov, A. M., & Thompson, C. 2007, ApJ, 657, 967
Burwitz, V., Zavlin, V., Neuhauser R., et al. 2001, A&A, 379, L35
Burwitz, V., Haberl, F., Neuhauser, R., et al. 2003, A&A, 399, 1109
Cheng, K. S., Ho, C., & Ruderman, M. A. 1986, ApJ, 300, 500
Fernandez, R., & Thompson, C. 2007, ApJ, 660, 615
Goldreich, P., & Julian, W. H. 1969, ApJ, 157, 869
Haberl, F. 2007, ApSS, 308, 181
Herold, H. 1979, Phys. Rev. D, 19, 2868
Ho, W. C. G., Kaplan, D. L., Chang, P., et al. 2007, MNRAS, 357, 821
Kaplan, D. L., & van Kerkwijk, M. H. 2009, ApJ, 692, L62
Kaspi, V. M., Roberts, M. S. E., & Harding, A. K. 2006, Isolated neutron stars, eds. W. Lewin, & M. van der Klis (Cambridge, UK: Cambridge Univ. Press) (arXiv: astro-ph/0402136)
Liu, D. B., Chen, L., Ling, J. J., et al. 2004, A&A, 417, 381
Luo, Q., & Melrose, D. 2007, MNRAS, 378, 1481
Lyutikov, M., & Gavriil, F. P. 2006, MNRAS, 368, 690
Lyutikov, M. 2008, AIP Conf. Proc., 968, 77 (arXiv: 0708.1024)
McLaughlin, M. A., Lyne, A. G., Lorimer D. R., et al. 2006, Nature, 439, 817
McLaughlin, M. A., Lyne, A. G., Keane, E. F., et al. 2009, MNRAS, 400, 1431
Morrison, R., & McCammon, D. 1983, ApJ, 270, 119
Motch, C., Zavlin, V., & Haberl, F. 2003, A&A, 408, 323
Nobili, L., Turolla, R., & Zane, S. 2008, MNRAS, 386, 1527
Padmanabhan, T. 2000, Theoretical astrophysics (Cambridge: Cambridge)
Pathria, R. K. 2003, Statistical mechanics (2nd ed.; Singapore: Elsevier)
Rea, N., Zane, S., Turolla, R., et al. 2008, ApJ, 686, 1245
Ross, R., Weaver, R., McCray, R. 1978, ApJ, 219, 292
Ruderman, M. A., & Sutherland, P. G. 1975, ApJ, 196, 51
Ruderman, M. 2003, arXiv: astroph/0310777
Rybicki, G. B., & Lightman, A. P. 1979, Radiative process in astrophysics (New York: Wiley Interscience)
Sunyaev, R. A., & Titarchuk, L. G. 1980, A&A, 86, 121
Thompson, C., Lyutikov, M., & Kulkarni, S. R. 2002, ApJ, 574, 332
Tong, H., & Peng, Q. H. 2007, ChJAA (Chin. J. Astron. Astrophys.), 7, 809
Tong, H., Peng, Q. H., & Bai, H. 2008, ChJAA (Chin. J. Astron. Astrophys.), 8, 269
Trümper, J. 2005, in NATO ASIB Proc. 210, The Electromagnetic Spectrum of Neutron Stars, 117 (arViv: astro-ph/0502457)
van Kerkwijk, M. H., & Kaplan, D. L. 2007, ApSS, 308, 191
Wang, F. Y. -H., Ruderman, M., Haplern, J. P., et al. 1998, ApJ, 498, 373
Xu, R. X. 2002, ApJ, 570, L65
Xu, R. X. 2003, ApJ, 596, L59
Xu, R. X. 2009, J. Phys. G: Nucl. Part. Phys., 36, 064010
You, J. H., Chen, J. F., Deng, J. S., et al. 1997, Phys. Lett. A, 232, 367
You, J. H. 1998, Radiative Process in Astrophysics (2nd ed.; Beijing: Scientific Press) (in Chinese)